

Spectroscopic studies of ferricyanide oxidation of *Azotobacter vinelandii* ferredoxin I

(iron–sulfur clusters/magnetic circular dichroism)

T. V. MORGAN[†], P. J. STEPHENS^{†‡}, F. DEVLIN[†], C. D. STOUT[§], K. A. MELIS[§], AND B. K. BURGESS[¶]

[†]Department of Chemistry, University of Southern California, Los Angeles, CA 90089-0482; [§]Department of Crystallography, University of Pittsburgh, Pittsburgh, PA 15260; and [¶]C. F. Kettering Research Laboratory, Yellow Springs, OH 45387

Communicated by Martin D. Kamen, September 22, 1983

ABSTRACT The $\text{Fe}(\text{CN})_6^{3-}$ oxidation of the crystallographically characterized $\{[3\text{Fe-3S}], [4\text{Fe-4S}]\}$ ferredoxin I of *Azotobacter vinelandii* has been studied using absorption, circular dichroism, magnetic circular dichroism, and EPR spectroscopies. A paramagnetic intermediate is observed en route to Fe–S cluster-free apoprotein, possessing an anisotropic $g \approx 2$ EPR signal, surviving to temperatures >77 K. This species is shown to result from 3-electron oxidation of the $[4\text{Fe-4S}]$ cluster, without modification of the $[3\text{Fe-3S}]$ cluster. However, it does not give rise to observable paramagnetic magnetic circular dichroism in the visible-near UV spectral region and is therefore neither an oxidized HIPIP $[4\text{Fe-4S}]$ cluster nor an oxidized $[3\text{Fe-3S}]$ cluster. We identify the paramagnetic species as a cysteinylsulfide radical formed on dissociation of an oxidized cysteinate and an oxidized sulfide ion from the $[4\text{Fe-4S}]$ cluster. This conclusion is consistent with the observed reaction stoichiometry, the spectroscopic results obtained, known EPR spectra of disulfide radicals, and the reconstitution of the native $[4\text{Fe-4S}]$ cluster by dithiothreitol alone. This reaction, earlier interpreted as a HIPIP-type oxidation, is a previously uncharacterized oxidation reaction of $[4\text{Fe-4S}]$ clusters.

The structure of *Azotobacter vinelandii* ferredoxin I (Fd I) has recently been determined by x-ray crystallography to a resolution of 2.0 Å (1, 2). [We follow the nomenclature of Yoch and Arnon (3). This protein has also been named *A. vinelandii* iron–sulfur protein III (4).] The structure shows two iron–sulfur clusters, 11 Å apart, containing four and three iron atoms respectively. The $[4\text{Fe-4S}]$ cluster is essentially identical to those previously characterized crystallographically in *Peptococcus aerogenes* ferredoxin (ref. 5 and references therein) and *Chromatium vinosum* high-potential iron protein (HIPIP) (ref. 6 and references therein), involving a cubal Fe_4S_4 core (S^* , inorganic sulfide) ligated by four cysteine residues. The $[3\text{Fe-3S}]$ cluster is a novel structure. The Fe_3S_3 core is nearly planar; ligation is by five cysteine residues and one other ligand, possibly H_2O .

Mössbauer spectroscopy (7) shows that the $[3\text{Fe-3S}]$ cluster is paramagnetic and the $[4\text{Fe-4S}]$ cluster is diamagnetic in the oxidation level as isolated. The $[3\text{Fe-3S}]$ cluster is therefore associated with the nearly isotropic $g \approx 2.0$ EPR signal observed at liquid helium temperatures (8). Sodium dithionite is reported to reduce the $[3\text{Fe-3S}]$ cluster to a state that is paramagnetic but EPR-silent, the $[4\text{Fe-4S}]$ cluster being unaffected (7).

The reducible $[3\text{Fe-3S}]$ cluster was earlier identified (8) as a HIPIP-type $[4\text{Fe-4S}]$ cluster, on the basis of its $g \approx 2.0$ EPR signal when oxidized. (A HIPIP-type $[4\text{Fe-4S}]$ cluster is defined to exhibit redox between 3^+ and 2^+ oxidation levels of the $[\text{Fe}_4\text{S}_4]^{n+}$ cluster core. In contrast, a low-potential

$[4\text{Fe-4S}]$ cluster operates between 2^+ and 1^+ levels.) In the same work, the $[4\text{Fe-4S}]$ cluster was also characterized as a HIPIP-type cluster, as a result of the development of additional $g \approx 2.0$ EPR intensity on $\text{Fe}(\text{CN})_6^{3-}$ oxidation. Redox potentials of -424 mV and $+320$ mV were reported (3, 8, 9) for the two clusters, suggesting an enormous (>700 mV) variability in the potentials of HIPIP clusters with protein environment. This conclusion is now unsupported, as a result of the identification of the $[3\text{Fe-3S}]$ cluster. In addition, recent work (10–12) has shown that oxidation of proteins containing $[4\text{Fe-4S}]$ clusters can generate $[3\text{Fe}]$ clusters, raising the possibility that the $[4\text{Fe-4S}]$ cluster of Fd I is also not of the HIPIP type and that $\text{Fe}(\text{CN})_6^{3-}$ oxidation is producing a second $[3\text{Fe}]$ cluster. [The $[3\text{Fe}]$ clusters in proteins other than Fd I may differ in stoichiometry and structure from that in Fd I. In beef heart aconitase, the stoichiometry is reported to be consistent with a $[3\text{Fe-4S}]$ cluster (13).]

We report preliminary results of spectroscopic studies that show that the $\text{Fe}(\text{CN})_6^{3-}$ oxidation of Fd I involves a new, previously unrecognized, oxidation reaction of $[4\text{Fe-4S}]$ clusters.

EXPERIMENTAL METHODS

Fd I was purified as described (1, 2, 14) or by a modified procedure in which the butanol extraction is replaced by the first steps of nitrogenase purification (15). All Fd I was crystallized in either the tetragonal or triclinic form (14). The A_{280}/A_{400} ratios were consistent with the best values reported previously (1–3).

Absorption spectra were measured on a Cary 17 spectrometer. Circular dichroism (CD) and magnetic circular dichroism (MCD) were measured using a modified JASCO J-500C spectropolarimeter. Magnetic fields up to 30 kilogauss (kG) and sample temperatures down to 1.7 K were provided using an Oxford Instruments Spectromag 5 split-coil superconducting magnet system.

Room temperature absorption and CD measurements were carried out using small volume cylindrical cells with fused quartz windows (Optical Cell, Woodbine, MD). For anaerobic measurements, the cells were loaded in an O_2 -free (<0.5 ppm O_2) glove box (Vacuum Atmospheres, Hawthorne, CA) into an o-ring-sealed holder with fused quartz windows. Low-temperature absorption, CD, and MCD measurements were carried out using glycerol glasses. The protein solution was diluted 1:1 with glycerol, placed in a cell containing two fused quartz windows separated by a gasket ≈ 1 mm thick and frozen in liquid nitrogen. When necessary this was carried out in the O_2 -free glove box. Room temperature path lengths were measured using both a micrometer and absorption and CD spectra.

The publication costs of this article were defrayed in part by page charge payment. This article must therefore be hereby marked "advertisement" in accordance with 18 U.S.C. §1734 solely to indicate this fact.

Abbreviations: CD, circular dichroism; MCD, magnetic circular dichroism; HIPIP, high-potential iron protein; Fd I, ferredoxin I.
[‡]To whom reprint requests should be addressed.

EPR spectra were obtained using a Varian E-12 spectrometer and an Oxford Instruments ESR-9 flow cryostat.

Unless otherwise indicated all Fd I solutions were in 100 mM potassium phosphate buffer (pH 7.5). Fd I concentrations were determined spectrophotometrically using $\epsilon_{400} = 29,800$ (W. V. Sweeney, personal communication). $K_3Fe(CN)_6$, sodium dithionite, dithiothreitol were from Mallinckrodt, Fisher, and Sigma, respectively. Concentrations of $Fe(CN)_6^{3-}$ and sodium dithionite solutions were determined spectrophotometrically using $\epsilon_{420} = 1020$ (16) and $\epsilon_{314} = 8000$ (17), respectively.

RESULTS

The room-temperature and pH 7.5 visible-near UV absorption and CD spectra of Fd I as isolated (henceforth referred to as oxidized Fd I, $Fd I_{ox}$) and their change on titration with $K_3Fe(CN)_6$ are shown in Fig. 1. At the concentrations used for optical spectroscopy (50–100 μM) and at ambient temperatures, the reaction of $Fe(CN)_6^{3-}$ with $Fd I_{ox}$ is slow, complete reaction typically requiring 0.5 to 2 hr. Equilibration is conveniently monitored using the CD spectrum. All spectra shown in Fig. 1 have been measured after equilibration.

The EPR spectrum of $Fd I_{ox}$ at 11 K is shown in Fig. 2; it broadens rapidly with increasing temperature and is undetectable at 50 K. On titration with $Fe(CN)_6^{3-}$, the 11 K EPR initially broadens and develops additional structure (8); subsequently, the intensity decreases to zero. The EPR created on $Fe(CN)_6^{3-}$ oxidation broadens relatively slowly with increasing temperature and remains observable above 77 K. A comparison of the temperature dependence of the EPR of $Fd I_{ox}$ and $Fe(CN)_6^{3-}$ -oxidized $Fd I_{ox}$ at a $Fe(CN)_6^{3-}/Fd I$ ratio of 3.3 is shown in Fig. 2. The change in the 50 K EPR spectrum on titration with $Fe(CN)_6^{3-}$ is shown in Fig. 3.

The optical and EPR spectra clearly indicate the existence of two phases in the reaction of Fd I with $Fe(CN)_6^{3-}$. In the

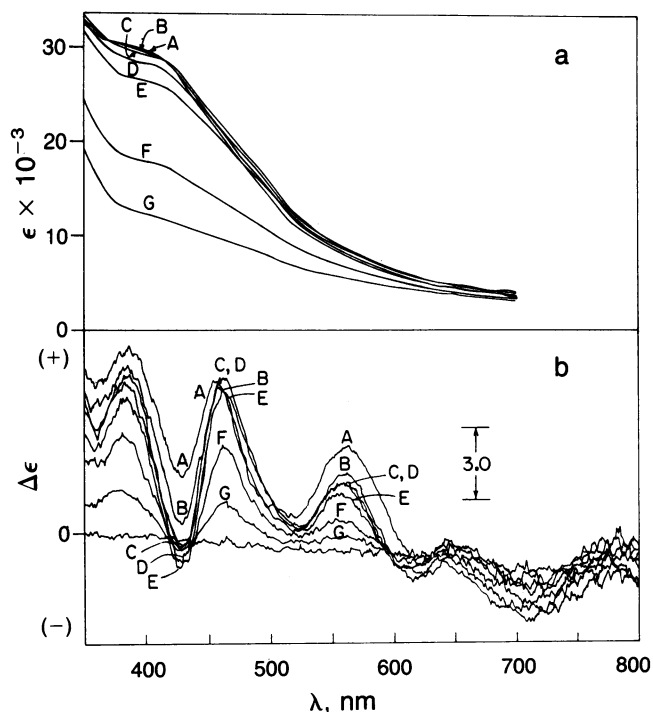


FIG. 1. (a) Absorption and (b) CD of $Fe(CN)_6^{3-}$ -oxidized $Fd I_{ox}$. $Fe(CN)_6^{3-}/Fd I_{ox}$ ratios are as follows: A, 0; B, 1.0; C, 2.1; D, 3.2; E, 5.3; F, 16; G, 21. $Fd I_{ox}$ is 0.057 mM in 100 mM phosphate buffer (pH 7.5). Spectra were run after equilibration (30–60 min). Spectra are not corrected for dilution, which is <3%.

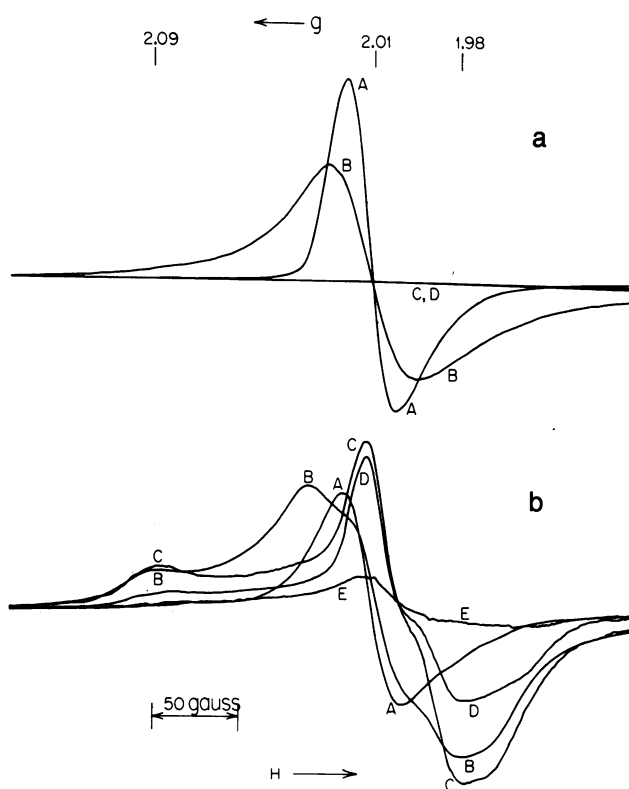


FIG. 2. EPR of (a) $Fd I_{ox}$ and (b) $Fe(CN)_6^{3-}$ -oxidized $Fd I_{ox}$ [$Fe(CN)_6^{3-}/Fd I_{ox}$ ratio is 3.3]. Temperatures are as follows (in K): A, 11; B, 20; C, 30; D, 50; E, 77. Gains are A, 50; B, 500; C, D, and E, 1000. Microwave frequency is 9.385 GHz, power is 2 mW, and modulation is 10 G. $Fd I_{ox}$ is 0.058 mM in 100 mM phosphate buffer (pH 7.5). In b, incubation after mixing was for 1 hr at ambient temperature.

first phase, the absorption changes very little, the CD changes substantially in both shape and magnitude, and a new EPR signal is created. In the second phase, absorption, CD and EPR decrease essentially monotonically to zero. The two reaction phases overlap somewhat; however, as is most clearly shown by the 50 K EPR titration, the first involves a 3-electron reaction. The paramagnetic product of the first reaction will be referred to as $Fd I'_{ox}$.

The liquid helium temperature MCD spectrum of $Fd I_{ox}$ exhibits paramagnetic behavior (18, 19). The visible-near UV MCD at 28.1 kG and 1.78 K is shown in Fig. 4. The spectrum of $Fe(CN)_6^{3-}$ -oxidized $Fd I_{ox}$ at a $Fe(CN)_6^{3-}/Fd I$ ratio of 3.0 is also shown; within experimental error, no change in MCD occurs on $Fe(CN)_6^{3-}$ oxidation.

As gauged by the appearance of the characteristic absorption, EPR, and low temperature MCD of $Fe(CN)_6^{3-}$, the reaction with $Fd I_{ox}$ after equilibration completely consumes the added $Fe(CN)_6^{3-}$ up to $Fe(CN)_6^{3-}/Fd I$ ratios of >20.

We have examined the effects of large excesses of ascorbate and of dithiothreitol on the absorption, CD and EPR of $Fe(CN)_6^{3-}$ -oxidized $Fd I_{ox}$. Neither reagent affects the spectra of $Fd I_{ox}$. At any $Fe(CN)_6^{3-}/Fd I$ ratio, the effects of ascorbate are very minor, and in no case are the spectroscopic changes induced by $Fe(CN)_6^{3-}$ reversed. By contrast, in the initial phase of $Fe(CN)_6^{3-}$ oxidation (up to a $Fe(CN)_6^{3-}/Fd I$ ratio of ≈ 2), changes in CD and EPR are totally reversed (within experimental error) by dithiothreitol on incubation for 2 hr; at any $Fe(CN)_6^{3-}/Fd I$ ratio, dithiothreitol removes the 50 K EPR signal.

The reaction of $Fd I_{ox}$ with $Fe(CN)_6^{3-}$ in the presence and in the absence of O_2 produces very similar spectral changes. Small differences were observed, however, in both optical and EPR spectra, indicating some incursion of O_2 into the

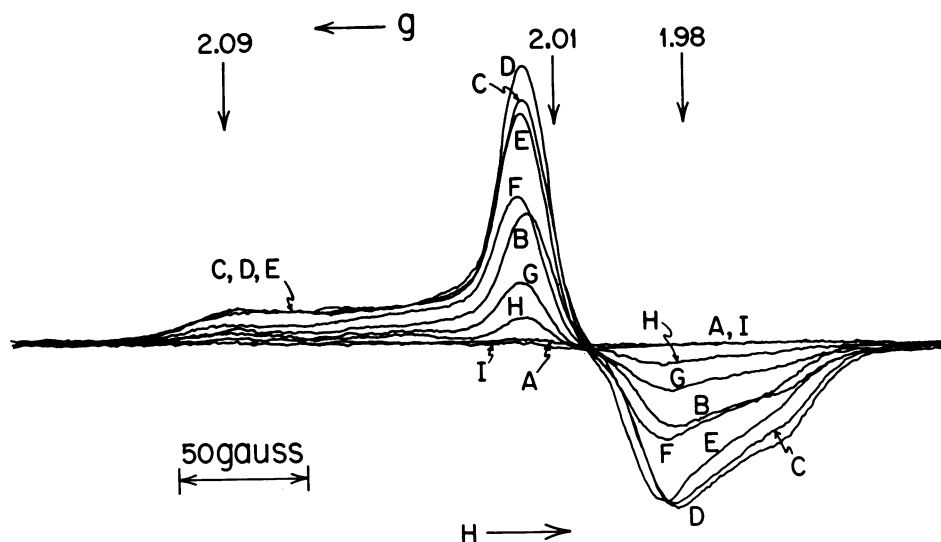


FIG. 3. EPR of $\text{Fe}(\text{CN})_6^{3-}$ -oxidized Fd I_{ox} at 50K. $\text{Fe}(\text{CN})_6^{3-}/\text{Fd I}_{\text{ox}}$ ratios are as follows: A, 0; B, 1.0; C, 2.0; D, 3.0; E, 4.9; F, 9.9; G, 15; H, 20; I, 30. Solutions were mixed and incubated 1.5 hr at ambient temperature prior to freezing. Spectra are not corrected for dilution, which is always $<2\%$. Fd I_{ox} is 0.044 mM in 100 mM phosphate buffer (pH 7.5). Microwave frequency is 9.386 GHz, power is 2 mW, modulation is 10 G, and gain is 1.25×10^3 .

reaction. All experimental data reported here were obtained under strictly anaerobic conditions.

No precipitation of either protein or inorganic material was observed during $\text{Fe}(\text{CN})_6^{3-}$ oxidation of Fd I_{ox} .

DISCUSSION

The visible-near UV absorption spectrum and 11 K EPR spectrum of Fd I_{ox} are in good agreement with spectra in the literature (3, 8). Neither CD nor MCD spectra of Fd I have previously been published. The absorption and CD of Fd I_{ox} are the composite of the contributions of the [3Fe-3S] and [4Fe-4S] cluster. The EPR and paramagnetic MCD spectra arise solely from the [3Fe-3S] cluster, since the [4Fe-4S] cluster is diamagnetic. Both EPR and MCD spectra are very similar to those reported for other oxidized [3Fe] clusters. [EPR spectra of [3Fe] clusters, independently characterized by either Mössbauer spectroscopy or low-temperature MCD, have been observed in *Desulfovibrio gigas* ferredoxin II (20), beef heart aconitase (21), and $\text{Fe}(\text{CN})_6^{3-}$ -oxidized

Clostridium pasteurianum ferredoxin (10). MCD spectra of [3Fe] clusters have been reported for *D. gigas* ferredoxin II (22) and $\text{Fe}(\text{CN})_6^{3-}$ -oxidized *C. pasteurianum* ferredoxin (10).]

The changes in the absorption, CD and EPR spectra of Fd I_{ox} on titration with $\text{Fe}(\text{CN})_6^{3-}$ reveal a paramagnetic intermediate oxidation product ($\text{Fd I}'_{\text{ox}}$) en route to Fe-S cluster-free apoprotein. Formation of $\text{Fd I}'_{\text{ox}}$ involves removal of three electrons from Fd I_{ox} . The changes in CD and EPR are initially linear with added $\text{Fe}(\text{CN})_6^{3-}$ concentration, and then exhibit curvature due to the overlapping of the further oxidation reaction of $\text{Fd I}'_{\text{ox}}$. There is as yet no clear evidence for additional intermediates.

The formation of $\text{Fd I}'_{\text{ox}}$ involves reaction at the [4Fe-4S] cluster. This is most clearly shown by the identity of the low-temperature MCD spectrum of Fd I_{ox} and $\approx 3:1$ $\text{Fe}(\text{CN})_6^{3-}$ -oxidized/ Fd I_{ox} (Fig. 4). We now refer to the [4Fe-4S] cluster oxidation product occurring in $\text{Fd I}'_{\text{ox}}$ as [4Fe-4S]'. The preceded reactions that were initially anticipated are either (i) HIPIP-type oxidation, resulting in a

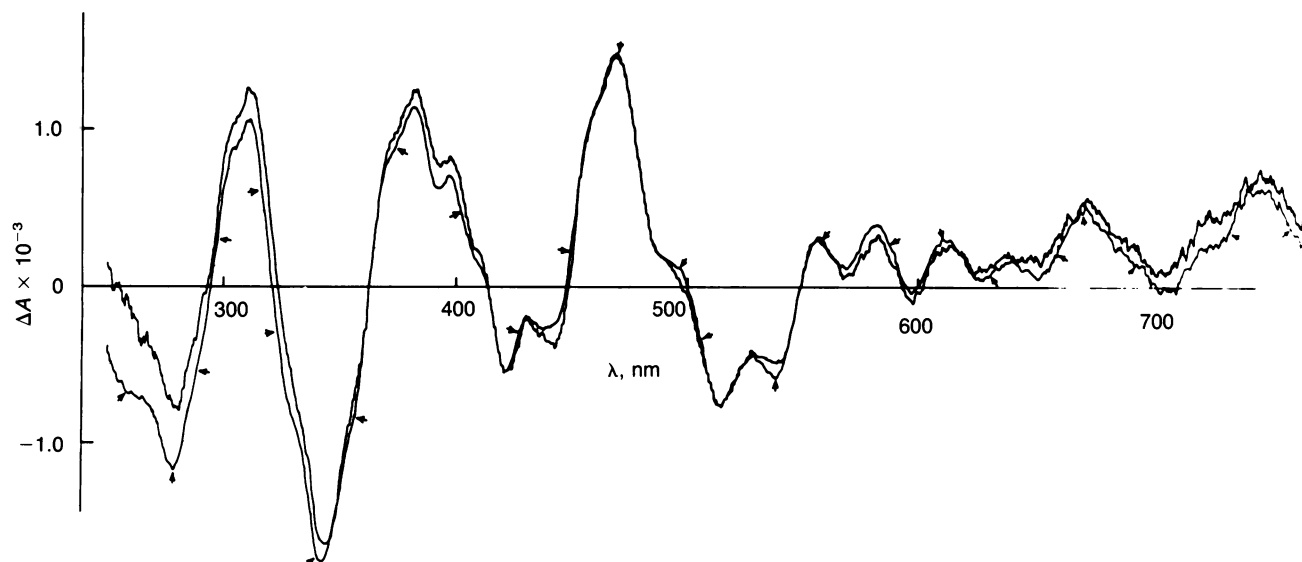


FIG. 4. MCD of Fd I_{ox} (with arrows) and 3.0/1 $\text{Fe}(\text{CN})_6^{3-}$ -oxidized Fd I_{ox} (without arrows) at 1.78K and +28.1 kG. Fd I_{ox} and $\text{Fe}(\text{CN})_6^{3-}$ -oxidized Fd I_{ox} are both 0.081 mM in 100 mM phosphate buffer (pH 7.5) diluted 50:50 (vol/vol) by glycerol. Path lengths are 1.02 and 1.10 mm, respectively.

[4Fe-4S]³⁺ cluster, or (ii) conversion to a [3Fe] cluster in its oxidized state. The former is a one-electron, reversible redox reaction, leading to a paramagnetic cluster typically exhibiting an axial EPR spectrum with *g* values significantly above 2 (23) and a characteristic paramagnetic MCD spectrum (24). The latter (10–12) is an irreversible reaction in which Fe and (maybe) S are lost from the cluster, leading to a paramagnetic cluster, characterized by a near-isotropic EPR signal with *g* ≈ 2.0 (10, 20, 21) and a characteristic paramagnetic MCD spectrum (10, 22). The EPR and low-temperature MCD spectra of the only [3Fe] cluster crystallographically characterized to date—that in Fd I itself—are shown in Fig. 2 and 4.

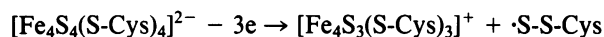
Despite the long-standing assertion by Yoch and co-workers [8, 9, 25] that the Fe(CN)₆³⁻-oxidation of Fd I_{ox} is of the HIPIP type, all available evidence is inconsistent with this possibility. First, the formation of [4Fe-4S]' involves three, and not one, electrons. Second, the change in absorption during the initial oxidation phase is so small that it is difficult to measure reliably. In contrast, HIPIP exhibits a large increase in absorption on oxidation (26, 27). Third, the EPR *g* values of [4Fe-4S]' do not resemble those of HIPIP (23). Fourth, an oxidized HIPIP cluster should contribute an additional paramagnetic MCD spectrum, equal in order of magnitude and quite different in structure to that of the [3Fe-3S] cluster. This is definitively absent, as shown in Fig. 4. Fifth, the Fe(CN)₆³⁻ oxidation is not reversed by ascorbate, which shows that the reaction is not a simple reversible redox reaction. Sixth, Fe(CN)₆³⁻ oxidation of Fd I_{ox} is much slower than that of HIPIP, despite the greater accessibility of the [4Fe-4S] cluster in the former (3, 4, 6).

The possibility that the Fe(CN)₆³⁻ oxidation of Fd I_{ox} involves conversion of the [4Fe-4S] cluster to a [3Fe] cluster is also inconsistent with our observations. First, as is clear from Fig. 2, the shape and temperature dependence of the EPR signal created by Fe(CN)₆³⁻ oxidation is quite different from that of the [3Fe-3S] cluster and does not simply add a second signal of similar shape and temperature dependence. Second, creation of a second [3Fe] cluster should double the paramagnetic MCD while retaining essentially the same structure. This is quite different from the actual negative result of Fig. 4.

It must be concluded, therefore, that the Fe(CN)₆³⁻ reaction of Fd I_{ox} falls into neither class of precedented reaction. The identification of the nature of the reaction was arrived at as follows. First, the low-temperature MCD spectrum of Fe(CN)₆³⁻-oxidized Fd I_{ox} shows no sign of paramagnetic MCD due to the EPR-active species [4Fe-4S]' created by Fe(CN)₆³⁻. This shows that the electron spin responsible for the EPR signal is not significantly coupled to the Fe-containing cluster, and that the latter is diamagnetic, since a paramagnetic Fe-S cluster must generate a substantial visible-near UV paramagnetic MCD spectrum. In addition, the paramagnetic moiety must either exhibit no electronic transitions in the spectral region studied or these must have extremely small paramagnetic MCD. The latter is possible if spin-orbit coupling is small in the species involved. Altogether, therefore, the low-temperature MCD spectrum suggests a dissociation of an organic radical species, not directly coupled to the Fe-S cluster, which remains diamagnetic.

Since the [4Fe-4S] cluster involves binding of Fe by S²⁻ and cysteine only, an obvious possibility is the formation of a sulfur-containing radical. A reasonable hypothesis regarding formation of such a radical can be based on the analysis of Petering *et al.* (28) of Fe(CN)₆³⁻ oxidation of various Fe-S proteins. This involved (i) oxidation of Fe²⁺, S²⁻ and cysteine (Cys-S⁻) to Fe³⁺, S⁰, and cysteinyl (Cys-S·) oxidation levels, respectively; (ii) loss of Fe from the protein; (iii) retention of S⁰ by the protein in the form of trisulfide links (Cys-S-S-S-Cys). In the present system, the assumptions

that initial reaction of Fe(CN)₆³⁻ is with one S²⁻ and one cysteine residue and that during oxidation the Fe-cysteine bond is broken, S⁰ leaves the cluster, and the resulting cysteinyl radical and S⁰ atom combine to form a cysteinyl disulfide radical (Cys-S-S·) provide a reaction



consistent with the observed stoichiometry and spectroscopy, as well as an intermediate consistent with the final products expected from the analysis of Petering *et al.* (28).

Thus, as long as the Fe-S cluster retains the formal oxidation level corresponding to 2Fe²⁺ and 2Fe³⁺ ions, the reaction involves three-electron oxidation, as observed. If the Cys-S-S· radical is sufficiently detached from the residual [Fe₄S₃(S-Cys)₃] cluster that covalent interaction is negligible and if the Fe-S cluster remains diamagnetic, as well as even-electron, then it is to be expected spectroscopically that (i) no visible-near UV paramagnetic MCD will be observed since Cys-S-S· should not have low-lying excited states and, in any case, would not be expected to generate large paramagnetic MCD; and (ii) the EPR signal of Cys-S-S· will persist to moderately high temperatures, since the mechanism responsible for the rapid broadening of Fe-S cluster EPR above liquid helium temperatures, involving low-lying Fe-S cluster excited states, is not available. The generation of Cys-S-S· is a reasonable intermediate in the formation of Cys-S-S-S-Cys, which requires only the oxidation of one further cysteine residue.

The hypothesis advanced above is supported by two direct lines of evidence. First, the cysteinyl disulfide radical has been identified among the products of radiation damage in γ -irradiated cysteine hydrochloride and cystine dihydrochloride (ref. 29 and references therein). It is, in fact, the most stable of these products, surviving at room temperature. Its EPR spectrum is observable at liquid nitrogen temperature and is an anisotropic spectrum with *g* values of ≈2.00, 2.02, and 2.06, not far from those observed in [4Fe-4S]'. (A simulation of the EPR line shape is required to determine precise *g* values for [4Fe-4S]'.) Second, the reconstitution of Fd I_{ox} from Fd I_{ox}, is predicted on the basis of the reconstitution of Fe(CN)₆³⁻-oxidized iron-sulfur apoproteins on addition of dithiothreitol and Fe²⁺, observed by Petering *et al.* (28). Dithiothreitol is able to regenerate S²⁻ and cysteine from cysteine trisulfide groups and should therefore do likewise from cysteinyl disulfide radicals. Since [4Fe-4S]' formation does not involve loss of Fe from the [4Fe-4S] cluster, only dithiothreitol should be required for reconstitution, as is observed.

Several further experimental observations are consistent with the above scheme. First, we have carried out comparative experiments using Co(phenanthroline)₃³⁺ in place of Fe(CN)₆³⁻ and obtained essentially identical results. The reaction is not specific to Fe(CN)₆³⁻, therefore, and the possibility that observed spectral changes (e.g., in the EPR spectrum) are due to an inorganic biproduct, specific to the oxidant used (e.g., Prussian blue or analogous complexes) can be ruled out. Second, the slow rate of the oxidation is consistent with a reaction involving considerable structural reorganization. Third, the insignificant change in absorption on formation of Fd I_{ox} is consistent with the retention of the initial Fe content of Fd I_{ox}, because in oxidative situations loss of absorbance in Fe-S clusters usually reflects loss of Fe. Fourth, up to a Co(phenanthroline)₃³⁺/Fd I_{ox} ratio of 6, no loss in Fd I Fe content is detected by direct analysis.

The demonstration that the [4Fe-4S] cluster of Fd I is not a HIPIP-type cluster leads to the possibility that it is a low-potential cluster, analogous to those of bacterial ferredoxins (30). Dithionite reduction at pH 7.5 causes loss of the EPR signal of Fd I_{ox} due to reduction of the [3Fe-3S] cluster, but

it does not yield a “ $g = 1.94$ ” signal, characteristic of reduced $[4\text{Fe-4S}]^{1+}$ clusters. However, reduction at pH 8.8 does yield a new signal, quite similar in shape and g values to those observed in reduced *Bacillus polymyxa* ferredoxins I and II (31) and the intermediate, one-cluster-reduced *C. pasteurianum* ferredoxin (30); its intensity corresponds to $\approx 25\%$ reduction. The simplest explanation for this signal is the reduction of the $[4\text{Fe-4S}]$ cluster, the lower reduction potential of sodium dithionite at pH 8.8, as compared to pH 7.5, accounting for the observation of the signal only at the more alkaline pH. However, it is also possible that at pH 8.8 the $[3\text{Fe-3S}]$ cluster is converted to a $[4\text{Fe-4S}]$ cluster and that the “ $g \approx 1.94$ ” EPR arises from the reduced state of a $\{2[4\text{Fe-4S}]\}$ protein. A precedent for such a reaction is provided by the activation of beef heart aconitase by sodium dithionite alone (11), since activation involves conversion from a $[3\text{Fe}]$ to a $[4\text{Fe-4S}]$ cluster. Experiments are in progress to distinguish these two possibilities.

The lowest redox potentials observed to date in $[4\text{Fe-4S}]$ clusters lie in the range -450 to -500 mV (25, 30). It appears that the potential of the $[4\text{Fe-4S}]$ cluster in Fd I is even lower. The physiological significance of this result remains to be established. Fd I is known to mediate electron transport to nitrogenase (32), an enzyme functioning at extremely reductive potentials.

This work was supported by the National Institutes of Health.

- Ghosh, D., Furey, W., O'Donnell, S. & Stout, C. D. (1981) *J. Biol. Chem.* **256**, 4185–4192.
- Ghosh, D., O'Donnell, S., Furey, W., Robbins, A. H. & Stout, C. D. (1982) *J. Mol. Biol.* **158**, 73–109.
- Yoch, D. C. & Arnon, D. I. (1972) *J. Biol. Chem.* **247**, 4514–4520.
- Shethna, Y. I. (1970) *Biochim. Biophys. Acta* **205**, 58–62.
- Adman, E. T., Sieker, L. C. & Jensen, L. H. (1976) *J. Biol. Chem.* **251**, 3801–3806.
- Freer, S. T., Sieker, L. C. & Jensen, L. H. (1976) *J. Biol. Chem.* **251**, 3801–3806.
- Emptage, M. H., Kent, T. A., Huynh, B. H., Rawlings, J., Orme-Johnson, W. H. & Munck, E. (1980) *J. Biol. Chem.* **255**, 1793–1796.
- Sweeney, W. V., Rabinowitz, J. C. & Yoch, D. C. (1975) *J. Biol. Chem.* **250**, 7842–7847.
- Yoch, D. C. & Carithers, R. P. (1978) *J. Bacteriol.* **136**, 822–824.
- Thomson, A. J., Robinson, A. E., Johnson, M. K., Cammack, R., Rao, K. K. & Hall, D. O. (1981) *Biochim. Biophys. Acta* **637**, 423–432.
- Kent, T. A., Dreyer, J. L., Kennedy, M. C., Huynh, B. H., Emptage, M. H., Beinert, H. & Munck, E. (1982) *Proc. Natl. Acad. Sci. USA* **79**, 1096–1100.
- Moura, J. J. G., Moura, I., Kent, T. A., Lipscomb, J. D., Huynh, B. H., LeGall, J., Xavier, A. V. & Munck, E. (1982) *J. Biol. Chem.* **257**, 6259–6267.
- Beinert, H., Emptage, M. H., Dreyer, J. L., Scott, R. A., Hahn, J. E., Hodgson, K. O. & Thomson, A. J. (1983) *Proc. Natl. Acad. Sci. USA* **80**, 393–396.
- Stout, C. D. (1979) *J. Biol. Chem.* **254**, 3598–3599.
- Burgess, B. K., Jacobs, D. B. & Stiefel, E. I. (1980) *Biochim. Biophys. Acta* **614**, 196–209.
- Schellenberg, K. A. & Hellerman, L. (1958) *J. Biol. Chem.* **231**, 196–209.
- Dixon, M. (1971) *Biochim. Biophys. Acta* **226**, 241–258.
- Stephens, P. J. (1974) *Annu. Rev. Phys. Chem.* **25**, 201–232.
- Stephens, P. J. (1976) *Adv. Chem. Phys.* **25**, 197–264.
- Cammack, R., Rao, K. K., Hall, D. O., Moura, J. J. G., Xavier, A. V., Bruschi, M., LeGall, J., Deville, A. & Gayda, J. P. (1977) *Biochim. Biophys. Acta* **490**, 311–321.
- Ruzicka, F. J. & Beinert, H. (1978) *J. Biol. Chem.* **253**, 2514–2517.
- Thomson, A. J., Robinson, A. E., Johnson, M. K., Moura, J. J. G., Moura, I., Xavier, A. V. & LeGall, J. (1981) *Biochim. Biophys. Acta* **670**, 93–100.
- Antanaitis, B. C. & Moss, T. H. (1975) *Biochim. Biophys. Acta* **405**, 262–279.
- Johnson, M. K., Thomson, A. J., Robinson, A. E., Rao, K. K. & Hall, D. O. (1981) *Biochim. Biophys. Acta* **667**, 433–451.
- Yoch, D. C. & Carithers, R. P. (1979) *Microbiol. Rev.* **43**, 384–421.
- Dus, K., Deklerk, H., Sletten, K. & Bartsch, R. G. (1967) *Biochim. Biophys. Acta* **140**, 291–311.
- Stephens, P. J., Thomson, A. J., Dunn, J. B. R., Keiderling, T. A., Rawlings, J., Rao, K. K. & Hall, D. O. (1978) *Biochemistry* **17**, 4770–4778.
- Petering, D., Fee, J. A. & Palmer, G. (1971) *J. Biol. Chem.* **246**, 643–653.
- Gordy, W. (1980) *Theory and Applications of Electron Spin Resonance* (Wiley, New York), Ch. 6 and 7.
- Sweeney, W. V. & Rabinowitz, J. C. (1980) *Annu. Rev. Biochem.* **49**, 139–161.
- Stombaugh, N. A., Burris, R. H. & Orme-Johnson, W. H. (1973) *J. Biol. Chem.* **248**, 7951–7956.
- Yates, M. G. (1977) in *Recent Developments in Nitrogen Fixation*, eds. Newton, W., Postgate, J. R. & Rodriguez-Barrueco, C. (Academic, New York), pp. 219–270.